Available online at www.sciencedirect.com

ScienceDirect

Procedia Manufacturing 47 (2020) 1381–1386

Procedia MANUFACTURING

www.elsevier.com/locate/procedia

23rd International Conference on Material Forming (ESAFORM 2020)

The influence of the kinematic hardening on the FEM simulation of Tension Levelling Process

Aitor Garcia[a], Javier Trinidad[a], Nagore Otegi[a], Joseba Mendiguren[a], Eneko Saenz de Argandoña[a], Elena Silvestre[b] and Lander Galdos[a,*]

[a]*Advanced Material Forming Processes research group, Mondragon Unibertsitatea, Loramendi 4, 20500 Arrasate-Mondragon, Spain*
[b]*Fagor Arrasate S. Coop., San Andres Auzoa 20, 20500 Arrasate-Mondragon, Spain*

* Corresponding author. Tel.: +34 943 79 47 00; fax: +34 943 15 36. *E-mail address:* lgaldos@mondragon.edu

Abstract

Tension levelling is used in the steel industry to remove shape defects present in cold rolled strip. This technology is increasingly being employed by steel makers to level AHSS steels, because conventional roll levelers are not able to correct explicit local errors like wavy edges and central buckles. In this study, the influence the hardening law has on the simulation of tension levelling processes using FEM is studied. Tension-compression tests have been performed in a DP1000 steel using several reversal cycles and a mixed nonlinear kinematic hardening law has been fitted to the experimental data using different amount of backstress tensors. It is observed that numerical results are influenced by the introduced hardening law and thus is an important input when simulating the tension levelling process.

Keywords: Tension Levelling; Kinematik hardening; Finite Element Modelling

1. Introduction

Shape defects resulting from differential elongation of parts of rolled strip is becoming an important industrial problem to guarantee high quality components. As the strip becomes thinner and the material is harder (non-ferrous materials in high temper and high strength steels) buckling is more likely to occur.

Nomenclature

σ	deviatoric stress tensor
X	deviatoric backstress tensor
σy	initial yield stress
R	isotropic hardening
ε_p	plastic strain
$\bar{\varepsilon_p}$	accumulated plastic strain
Q	material parameter
b	material parameter
C	material parameter
γ	material parameter

Local shape defects and strip flatness problems can be corrected using the roll levelling process unless the strip is so thin or defects are so big that the elongation caused by the rolls is not sufficient to produce significant yielding of the cross section. Deep details about this process are given in [1] where basic analytical models for the calculation of the plastified cross section ratio are presented and new concepts for modern design of roll levelers are shown.

Stretch levelling is an optional process to correct pronounced shape defects and homogenize the cross section residual stresses when roll levelling is not enough. During the process, the whole strip is uniaxially elongated using big size hydraulic grippers. However, high forces are needed and the process is pull-push, which limits the productivity of the line.

The tension levelling attempts to overcome the individual drawbacks of the two processes by combining them in such a

2351-9789
10.1016/j.promfg.2020.04.271

way that the strip is bent around a roll under superimposed tension. The superimposed tension causes the neutral bending line displacement and results in material elongation at comparatively lower applied tension (0.25-0.5 of the yield stress). The strip is then bent and stretched in the reverse direction and this is repeated until the desired strip elongation is achieved.

The tension in the strip is created by tension-rolls (bridles) with large diameters located at the inlet and the outlet of the line. Typically, these rolls are the only driven rolls in a tension levelling machine. The leveller unit itself consists of guiding-rolls, work-rolls and anti-camber and anti-coilset rolls (see Fig. 1). Guiding-roll diameters are larger compared to the work-rolls and are used mainly to guide the strip in the line without causing any yielding. The main plastic elongation of the strip is obtained in the work-rolls. The anti-camber and anti-coilset rolls are used to correct the tendency of the strip to curl at the line exit.

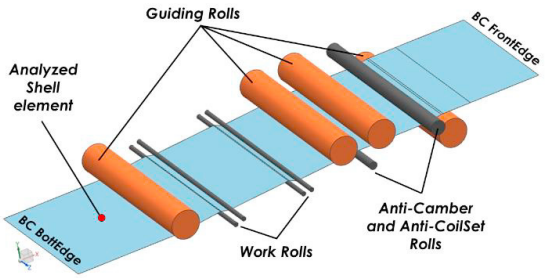

Fig. 1. Tension leveler unit.

Many Ultra High Strength Steels (UHSS) have been developed in the last two decades [2]. Among the different families, the Dual Phase steels are used for a big variety of applications, especially in the automotive sector. The use of thinner and thinner sheets aiming for a large weight reduction has increased the use of the tension levelling facilities in the finishing lines of these steels. However, almost all the tension levelling setups are based on rough calculations and previous industrial experiences, which have to be supplemented by trial and error procedures during the operation. Thus, precise and fast analytical models are needed to improve the design and the sizing of tension levelling machines. Unfortunately, the current process knowledge is well behind the needed level to develop such models.

As early as 1971, Robert and Sheppard and Roberts [3-4] developed advanced analytical models for the calculation of strip elongation and the evolution of through thickness stresses. Perfect elasto-plastic, isotropic and kinematic hardening material models were used for these calculations and validated in an experimental set-up. However, all the calculations in the existing analytical models depend on the curvature the strip adopts when crossing the tension levelling line and this information is unknown. Moreover, the shape of the strip significantly varies from the theoretical one when using high strength materials; the contact points between rolls and the strip are not located in the theoretical tangential points any more.

Advanced finite element models and design of experiment techniques were combined by Silvestre et al. to obtain an analytical model or a model of FE models to predict the strip curvature along a roll levelling line for a wide range of levellers and material thickness and properties [5]. The combination of these analytical rules together with an elastic-predictor plastic-corrector algorithm enabled the development of precise and fast analytical models for the optimization of roll levelling lines. The use of mixed kinematic hardening material models was needed for the correct comprehension of the process mechanism.

In this work, monotonic tensile tests and cyclic tension-compression tests have been used for the characterization of a DP1000 Dual Phase steel. Experimental tests have been fitted to a conventional isotropic hardening material model as well as to a mixed isotropic-kinematic hardening model with the ability to capture the Bauschinger effect the materials shows.

Finally, the tension levelling process has been simulated using different material models and the numerical results have been compared to increase the existing knowledge about the process mechanisms. The evolution of total and plastic strains, longitudinal through thickness stresses and roll forces have been evaluated with this aim.

The future validation of the numerical results using an experimental text bench being mounted in Mondragon University will enable the development of fast and accurate analytical models using the methodology used by Silvestre et al. in an earlier doctoral thesis for the roll levelling process.

2. Material characterization and modelling

2.1. Selected material and properties

A Dual Phase DP1000 with a thickness of 1.0 mm was used for the study. The mechanical properties of the material are shown in Table 1.

Table 1. Mechanical properties of DP1000 steel (ASTM E8 / E8M).

Yield strength (0.2% offset) (MPa)	Ultimate tensile Strength (MPa)	Elongation (%)
922.1	1055.7	8.7

2.2. Experimental methodology and results

Mechanical properties and the hardening behavior of the DP1000 material was obtained using monotonic tensile tests following the ASTM E8/E8M Standard. A strain rate of 0.001 s^{-1} was selected for the tests and 12.5 mm width standard specimen were used. For the monitoring of the longitudinal strain a contact extensometer was used.

For the characterization of the cyclic behavior of the material tension-compression tests were performed. The tension–compression test roved to be an appropriate experimental test to characterize the Bauschinger Effect and the identification of the material parameters of kinematic hardening laws [6]. Different authors have developed testing devices that avoid the specimen buckling during compression. Kuwabara et al. [7] proposed a sheet specimen which is sandwiched between two pairs of male and female dies.

Eggertsen and Mattiasson [8] developed similar equipment to prevent the buckling by applying a normal contact between the device and the specimen during testing. Yoshida et al. [9] suggested bonding five pieces of sheets together before machining them so that the thickness of the specimen was 5.0 mm. Bae and Hug [10] used as spring-loaded clamping device in various strain rates. A transparent wedge device was designed to prevent the buckling of thin sheets, allowing full field strain measurements of the specimen using digital imaging methods [11]. In the present study, a special tool to avoid buckling was also developed. The testing methodology and tool are described below.

The specimens were cut using a wire EDM from sheet in the rolling direction. They were rectangular with 1.5x12.5mm^2 cross section and a gauge length of 22.5mm. The geometry of the sample was specifically designed for this study, with the aim of using the developed anti bucking tool.

A servo-hydraulic MTS810 Material Test System was used for the experiments. Force data was acquired through an axial 100 kN load cell and strain data was measured with strain gages to obtain a continuous measurement. In particular, small deformation strain gages [12] were selected and had 5.33x5.84 mm^2 matrix length-width.

The strain gage was glued on the specimen in such a way that its position coincides with the hole of the upper die. In this way, the gage was not damaged. The wires passed through the hole of the upper die and were connected to the acquisition systems. Fig. 2 shows the experimental test equipment used with the tool to avoid buckling during the test. The specimen was clamped between the two holders leaving a 0.1 mm gap and was lubricated by Rhenus Fe1300 high viscosity lubricant to eliminate the influence of friction during the test [13].

The test started from a relaxed configuration, then the specimen was stressed in tension until 2% of deformation at a rate of 0.03 mm/s. In this point the load was reversed, and the sheet was discharged until a relaxed level of stress. Next, the specimen was loaded in compression until 2%. Once the maximum compression strain was achieved, the load was reversed again for discharging the accumulated stress in the specimen, closing the cyclic curve. This process was repeated for three cycles. These strain levels were selected because it is the typical strain range observed in tension levelers.

Three repetition were performed in both monotonic and cyclic tests.

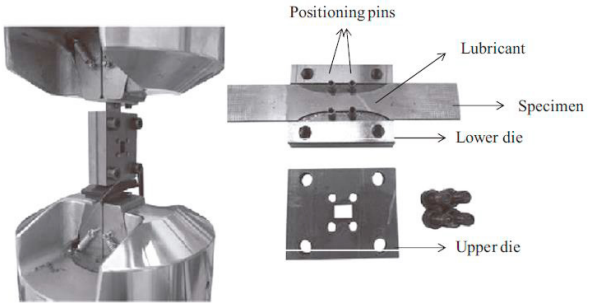

Fig. 2. Experimental test equipment.

The experimental flow curves obtained from the monotonic and cyclic tests are shown in Fig. 3.

The material showed a pronounced early reyielding and a prominent transient behavior. As it can be observed reyielding of the material after uniaxial tension starts almost at zero level of stress indicating that isotropic hardening of the material and yield surface expansion is negligible. The material behaves nearly as a purely kinetic hardening material.

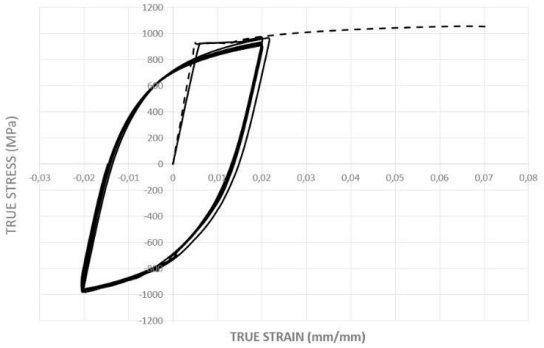

Fig. 3. Experimental flow curves from monotonic and cyclic tests.

2.3. Parameter identification of hardening models

The Chaboche and Lemaitre hardening model (1990) [14] was combined with the Von Mises yield criteria, as these are recommended for cyclic plasticity analyses and widely distributed in commercial FE-codes. The Von Mises yield criteria can be expressed:

$$\phi(\boldsymbol{\sigma}, \boldsymbol{X}, \sigma_y) = \sqrt{3/2\,(\boldsymbol{\sigma} - \boldsymbol{X}) : (\boldsymbol{\sigma} - \boldsymbol{X})} - \sigma_y - R \tag{1}$$

where $\boldsymbol{\sigma}$ denotes the deviatoric stress tensor, $\boldsymbol{X}$ is the deviatoric backstress tensor, σ_y is the initial yield stress and R is the isotropic hardening. An associated flow rule has been considered to define the plastic strain increment.

The Chaboche and Lemaitre hardening model is a mixed isotropic-kinematic hardening formulation. The nonlinear kinematic hardening describes the movement of the yield surface by means of the evolution of the backstress. The change in the size of the yield surface is related to the isotropic hardening and is introduced by means of the initial value of the yield strength σ_y and the isotropic variable R. In the proposed model, the evolution of the isotropic hardening is defined in function of the accumulated plastic strain $\mathrm{d}\bar{\varepsilon}_p$ by the following law:

$$\mathrm{d}R = b \cdot (Q - R) \cdot \mathrm{d}\bar{\varepsilon}p \tag{2}$$

where Q and b are material parameters of the model. The kinematic evolution of the yield surface, proposed by Chaboche et al. is presented in equation 3. This model is based on a decomposition of the non-linear kinematic hardening rule proposed by Armstrong and Frederik (1966). Chaboche decomposed a stable hysteresis curve in several parts and it was observed that increasing the material parameters of the hardening rule by the superposition of backstresses, a more accurate model was obtained [15].

$$d\boldsymbol{X} = \frac{2}{3}\cdot C\cdot d\boldsymbol{\varepsilon}_p - \gamma \boldsymbol{X}\cdot \mathrm{d}\bar{\varepsilon_p} \quad (3)$$

where C and γ are the material parameters to be fitted.

The parameter identification method consisted of an unconstrained non-linear optimization proposed by Nelder and Mead available at Matlab®. For the fitting procedure the plastic strain versus true stress monotonic and cyclic curves were used. The elastic strain was removed from the experimental curves using the 0.5% strain offset method.

The error function shown in equation 4 was minimized using all the experimental data of the three cyclic tests.

$$f_{obj} = \frac{1}{n}\sum_{i=1}^{n}\left|\sigma_i^{exp} - \sigma_i^{model}\right| \quad (4)$$

The fitting results using one backstress tensor are presented in Fig. 4 while Fig. 5 shows the results using two backstress tensors. In the same graphs, the isotropic Voce hardening model is also illustrated for comparison. The use of a mixed hardening law with three back stress tensors did not improved the fitting results and consequently it is not used in this work.

As can be observed, the model was able to predict the cyclic hardening of the material. Because the re-yielding of the material starts very early in the material, the Bauschinger effect is not completely captured by the model. In this regard, the best fitting is obtained not taking into account the isotropic hardening part of the mixed hardening model.

The transient behavior is not well described by the model with one back stress. This is significantly improved when using two back stress tensors. The material parameters for the different material models are summarized in Table 2.

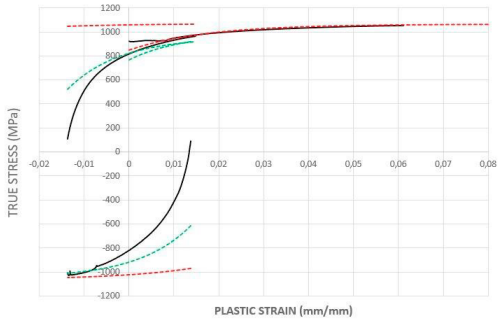

Fig. 4. Fitting of material models to experimental curves. Voce isotropic model in red and mixed Chaboche-Lemaitre model with one backstress tensor in green.

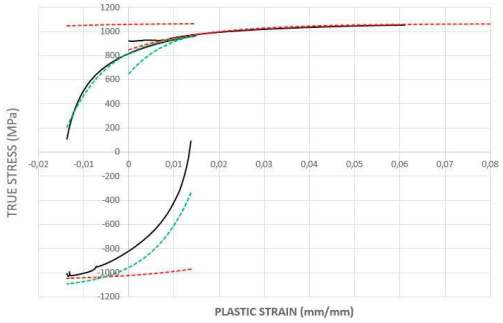

Fig. 5. Fitting of material models to experimental curves. Voce isotropic model in red and mixed Chaboche-Lemaitre model with two backstress tensors in green.

Table 2. Material parameters of the Isotropic model and the mixed Chaboche and Lemaitre hardening models with different amount of backstress tensors.

Voce isotopic hardening models				
σ_y	Q	b		
850	215	60		
Non-linear kinematic hardening model – One back stress tensor				
σ_y	C	γ		
765	18800	86		
Non-linear kinematic hardening model – Two back stress tensor				
σ_y	$C1$	$\gamma 1$	$C2$	$\gamma 2$
650	30000	110	13500	110

3. Numerical modelling

3.1. Numerical model description

Abaqus Explicit software was used for the tension levelling simulation. Work-rolls diameter is 30 mm with an intermesh (horizontal distance between work-rolls centers) of 60 mm. The Guiding rolls are sufficiently big to avoid the yielding of the strip and have a diameter of 200 mm. The anti-camber roll diameter is 55 mm and the anti-coilset roll diameter is 100 mm. The whole length of the levelling unit is 1950 mm. All the rolls are considered as rigid and are fixed in space. Because in the real machine the rolls rotate freely and are not driven, frictionless conditions were selected as contact behavior.

Shell elements with 15 integration point through thickness and with a mesh size of 3 mm were used to model the DP1000 strip as recommended by Huh et al. [16]. The strip width is 1000 mm. Two different models were used in the simulations. In the first model, a conventional Voce isotropic hardening law was used. In the second one, a non-linear kinematic hardening model with two backstress tensors was used.

At the two ends of the modelled strip, the bottom and front edges, either Dirichlet boundary conditions (i.e. strip speed values in agreement with the global strain level) or Neumann boundary conditions (strip tensions) have to be prescribed [17]. Two of these four values serve as input parameters to the system while the other two are essential results of the simulation. At least one boundary value has to be of Dirichlet type. In this study, the exit strip speed was set to be 2% higher than the entrance speed.

Work-rolls have a setting or penetration of 20 mm and the anti-camber and anti-coilset rolls were penetrated 10 mm each. The reference or zero machine was defined in the theoretical tangent point of rolls with a virtual perfectly tangent strip.

Aiming to understand the process mechanisms and the role of the material hardening law, the evolution of total longitudinal strains, plastic longitudinal strains and longitudinal through thickness stresses was monitored using a shell element located in the middle of the strip (see Fig. 1.). Roll forces were also evaluated since this is a critical output of the simulations for the correct sizing of an industrial line.

3.2. Numerical results

The total elongations suffered by the top, middle and bottom layers of the selected shell element are shown in Fig. 6 for the non-linear kinematic hardening and the isotropic hardening models.

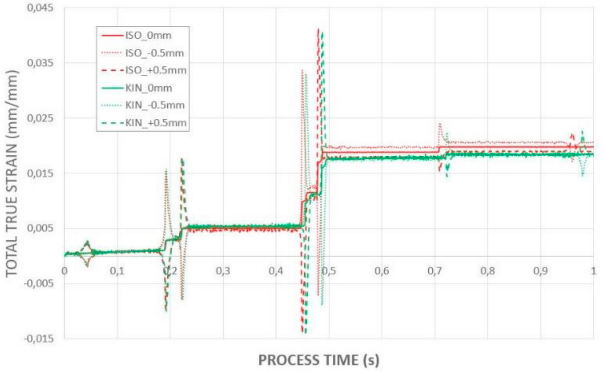

Fig. 6. Total elongation of the shell element top, middle and bottom layers.

Elongation profiles of the process clearly shows seven strain peaks. The first peak corresponds to the guiding roll and does not cause any plastic straining (the entrance total strain and the strain after the roll is identical). Second and third peaks correspond to the first pair of work-rolls and the fourth and fifth peak to the second pair of work-rolls. As it is observed a significant staining of the strip is achieved in these rolls being the increase of the second pair higher. Last two peaks correspond to the anti-camber and anti-coilset rolls, where a very small increase of the strip length is observed.

For better representation of the strains and stresses, through thickness total strains, plastic strains and axial stresses have been plotted in Fig. 7, Fig. 8 and Fig. 9 for four different levelling unit locations. These locations are the line entrance, the exit of the first pair of work-rolls (rolls 1 and 2), the second pair of work-rolls (rolls 3 and 4) and the exit of the line after the anti-camber and anti-coilset rolls.

Finally the reaction force of the rolls was monitored for the different numerical models. As it can be observed in Fig. 10 the forces are very similar for both cases.

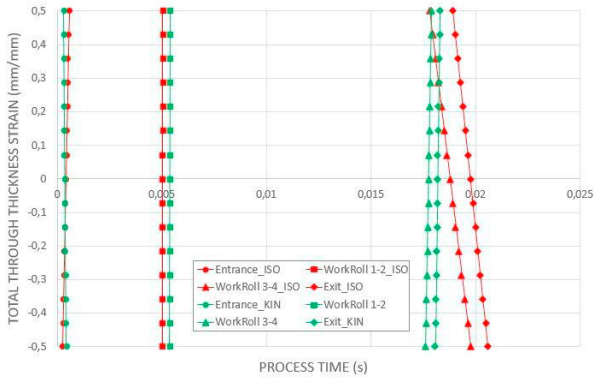

Fig. 7. Through thickness total strains for the selected locations of the levelling unit.

The computation time was 34% higher for the kinematic numerical model that the isotropic model. The isotropic model took 7 hours of computation in a conventional desktop computer.

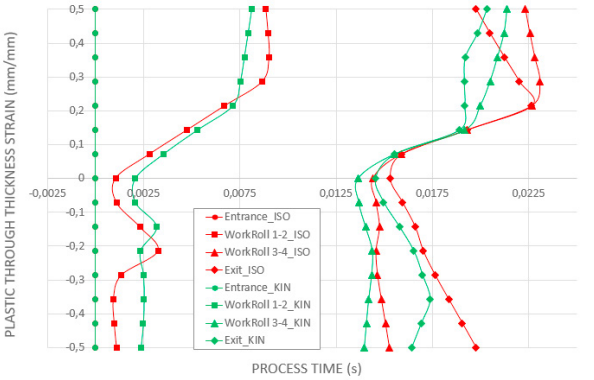

Fig. 8. Through thickness axial plastic strains for the selected locations of the levelling unit.

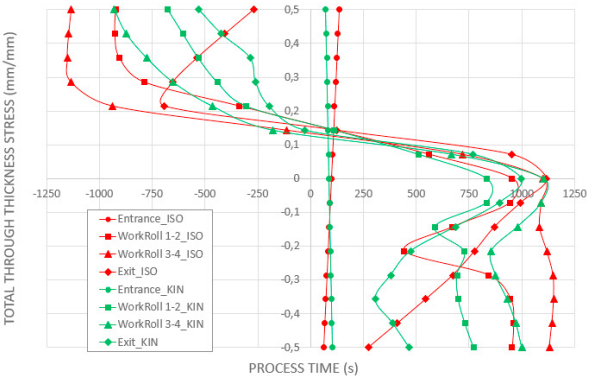

Fig. 9. Through thickness axial stresses for the selected locations of the levelling unit.

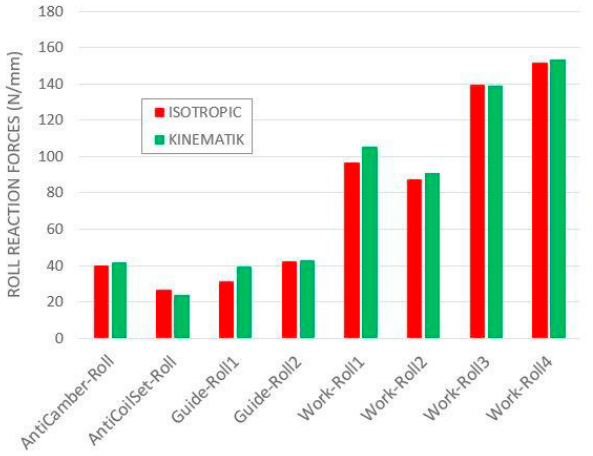

Fig. 10. Reaction forces of rolls for the different numerical models.

4. Discussion and conclusions

A non-linear kinematic hardening law has been used to capture the Bauschinger effect and transient behavior of a DP1000 Dual Phase steel. The material shows an almost pure kinematic hardening behavior with a negligible work hardening

and for this reason the isotropic hardening part of the combined mixed hardening model has not been used for the material model fitting. The material flow curve has also been fitted to a Voce hardening law to analyze the influence of the hardening law in the numerical results of the tension levelling process.

As it can be observed in the numerical results the total strain along the line is similar for both models although a slightly higher straining is observed for the isotropic hardening model. Similar behavior is observed if the through thickness total and plastic strains are analyzed. The shape of the strain profiles are similar for both models.

Axial stresses are in general lower for the kinematic model and the reaction forces of the rolls are very similar for both case. The higher forces are concentrated in the second pair of work rolls. This seems to be logical since in tension levelling lines there is a tension loss from the exit of the line to the entrance due to the elongation of the material.

The accuracy of the results needs to be confirmed by experimental testing and the authors are building an experimental device for this purpose. However, the hardening model appears to be not a significant input parameter for the estimation of relevant results like the strains evolution, the stress distribution and the roll forces. This statement needs to be confirmed by testing an extended range of materials.

Acknowledgements

Authors would like to thank the Basque Government for the economic support given to the ABT (Nueva máquina de Aplanado Bajo Tensión para materiales de alto límite elástico destinados a piezas estructurales y de la batería en coches coche eléctricos) research project and the FAGOR S.Coop. company for the economic and technical support.

References

[1] Silvestre E. Guía de aplanado por rodillos. Spain: Fagor Arrasate S. Coop.; 2019.

[2] Fonstein N. Advanced high strength sheet steels. Switzerland: Springer International Publishing; 2015.

[3] Roberts J. M. On the mechanics of the tension-levelling process. Journal of Institute of Metals 1971; 293.

[4] Roberts J. M. Continuum mechanics applied to the tension-levelling process; 1971.

[5] Silvestre E. Sheet metal roll levelling optimization by means of advanced numerical models and development of new concepts for last generation materials. Mondragon University; 2015.

[6] Silvestre E., Mendiguren J., Galdos L., Saenz de Argandoña E. Comparison of the hardening behaviour of different steel families: From mild and stainless steel to advanced high strength steels. International journal of mechanical sciences 2015;101:10-20.

[7] Kuwabara T. Elastic-plastic behavior of sheet metal subjected to in-plane reverse loading. In Proc. Plasticity'95, The 5th Int. Symposium on plasticity and its current applications 1995; 841-844.

[8] Eggertsen P. A., Mattiasson K. On the identification of kinematic hardening material parameters for accurate springback predictions. International Journal of Material Forming 2011; 4(2):103-120.

[9] Yoshida F., Uemori T. A model of large-strain cyclic plasticity describing the Bauschinger effect and workhardening stagnation. International journal of plasticity 2002; 18(5-6):661-686.

[10] Bae G. H., Huh H. Tension/compression test of auto-body steel sheets with the variation of the pre-strain and the strain rate. Transactions on engineering Sciences 2011;72:213-225.

[11] Magargee J., Cao J., Zhou R., McHugh M., Brink D., Morestin F. Characterization of tensile and compressive behavior of microscale sheet metals using a transparent microwedge device. Journal of Manufacturing Science and Engineering 2011; 133(6):064501.

[12] VishayMicro-measurements,Generalpurposestraingages – linear pattern; 2015.

[13] Mendiguren J., Galdos L., Sáenz de Argandoña E., Silvestre E. Ludwik's model parameter identification for v-bending simulations with Ti64 and MS1200. In Key Engineering Materials Trans Tech Publications 2012; 504:889-894.

[14] Lemaitre J., Chaboche J.L. Mechanics of solid materials. Cambridge university press 1994.

[15] Miyauchi K. Stress--Strain Relationship in Simple Shear of In-Plane Deformation for Various Steel Sheets. In Efficiency in Sheet Metal Forming, IDDRG 13 th Biennial Congress 1984; 360-371.

[16] Huh H., Lee H.W., Park S.R., Kim G.Y., Nam S.H. The parametric process design of tension levelling with an elasto-plastic finite element method. Journal of Materials Processing Technology 2001; 113(1-3):714-719.

[17] Steinwender L., Kainz A., Krimpelstätter K., Zeman K. Computational analysis of the curvature distribution and power losses of metal strip in tension levellers. In IOP Conference Series: Materials Science and Engineering 2010; 10:012135.